INCORPORATION OF HONEY-BASED PHENOLIC ACIDS INTO SHAPE MEMORY POLYMER FOAMS FOR USE AS ANTIMICROBIAL HEMOSTAT

An Undergraduate Research Scholars Thesis

by

KATHARYN GRANT

Submitted to the Undergraduate Research Scholars program at
Texas A&M University
in partial fulfillment of the requirements for the designation as an

UNDERGRADUATE RESEARCH SCHOLAR

Approved by Research Advisor: Dr. Duncan Maitland

May 2018

Major: Biomedical Engineering

TABLE OF CONTENTS

ABSTRACT

Incorporation of Honey-Based Phenolic Acids Into Shape Memory Polymer Foams for Use as Antimicrobial Hemostat

Katharyn Grant
Department of Biomedical Engineering
Texas A&M University

Research Advisor: Dr. Duncan Maitland
Department of Biomedical Engineering
Texas A&M University

Polyurethane shape memory polymer (SMP) foams are ultra-low density, "smart" materials that transition between a primary and secondary shape when exposed to a thermal stimulus. This material has the potential to be used in a new application as a hemostatic wound dressing. Honey-based phenolic acids are a class of naturally occurring antimicrobial substances produced by bees to protect their hives from harmful microbes in the environment. To tune the properties of SMP foams to best serve the proposed application, these honey-based phenolic acids will be incorporated into the polymer backbone to impart antimicrobial properties to the foams. An esterification reaction involving a phenolic acid and N,N,N,N'-tetrakis(2-hydroxypropyl) ethylene diamine (HPED) is carried out to produce a modified HPED molecule where one of the alcohol groups is replaced by the phenolic acid. SMP foams are then synthesized using hexamethylene diisocyanate (HDI), HPED, and varied amounts of triethanolamine (TEA) and the modified HPED-phenolic acid monomer. The resultant foams are characterized to determine their density, pore size, glass transition temperature (T_g), rate of thermal actuation, and antimicrobial properties.

ACKNOWLEDGEMENTS

I would like to thank Dr. Duncan Maitland for his mentorship and the opportunity to work in the Biomedical Device Laboratory. I would also like to thank Dr. Mary Beth Monroe for her guidance throughout the research and writing process, and Dr. Brandis Keller for her assistance editing. Finally, I would like to extend my gratitude to the other members of the Biomedical Device Laboratory for their support throughout this process.

NOMENCLATURE

SMP	Shape memory polymer
T_g	Glass transition temperature
HPED	N,N,N,N'-tetrakis(2-hydroxypropyl) ethylene diamine
TEA	Triethanolamine
FTIR	Fourier transform infrared
HDI	Hexamethylene diisocyanate
CA	Cinnamic acid
PAA	Phenylacetic acid
E. coli	Escherichia coli
Staph. epi.	Staphylococcus epidermis
HCA	N,N,N,N'-tetrakis(2-hydroxypropyl) ethylene diamine - cinnamic acid
HPAA	N,N,N,N'-tetrakis(2-hydroxypropyl) ethylene diamine - phenylacetic acid
DCC	N-N'-Dicyclohexylcarbodiimide
SEM	Scanning electron microscope
DSC	Differential scanning calorimeter
RO	Reverse osmosis
Nitinol	Nickel titanium
PBS	Phosphate buffered saline
LB	Lysogeny broth
CFU	Colony forming unit
P/S	Penicillin/Streptomycin

CHAPTER I

INTRODUCTION

Uncontrolled hemorrhage is the leading cause of preventable death on the battlefields in Iraq and Afghanistan, causing up to 80% of such deaths [1]. The dire effects of hemorrhage expand to include 30-40% of trauma mortality worldwide, with 33-56% occurring prior to the patient's arrival at a healthcare facility [2]. Current treatment options for battlefield injuries include the traditional tourniquet, and wound dressings made from a variety of materials, such as chitosan, fibrin, and oxidized cellulose [3, 4]. However, of these options, few provide the versatility required of a treatment used on the battlefield. One device garnering media attention is the XStat by RevMedx. This device uses oxidized cellulose to achieve hemostasis; however, it is difficult for surgeons to remove when the patient finally reaches a formal care center, and frequent dressing changes are required to reduce infection risks [4]. Thus, there is a need for a new, fast-acting treatment that will rapidly occlude the wound without significantly increasing surgical time.

Polyurethane shape memory polymer (SMP) foams have previously been used in embolic applications [5]. This porous material maintains its primary shape until it is heated above its glass transition temperature (T_g) and compressed into a secondary shape and cooled. If the foam is reheated to this T_g while in its secondary shape, the foam will thermally actuate and recover its primary shape. This material also possesses several other tunable thermal and mechanical properties that can be optimized for use as a prolonged field care hemostat.

SMP foams begin to actuate when exposed to temperatures equal to or greater than their T_g. The T_g of these foams can be tuned between 45-70°C in dry conditions [6]. Common U.S. war zones, such as Iraq and Afghanistan, have historically high temperatures, reaching up to 45°C in the summer months [7]. To avoid premature actuation of SMP foams in these environments, the dry T_g should exceed the average outdoor temperature. SMP foams additionally have a wet T_g that predominates after the foams have been plasticized with water. When a foam is exposed to blood, the water in the plasma interrupts hydrogen bonds between urethane links in the foam, lowering the T_g value. Ideally, the wet T_g will enable actuation of the foam at or below 37°C, or body temperature. When a foam begins to actuate, the time it takes to achieve full volume expansion can range between two minutes and twenty-four hours [8]. For a wound dressing, a more rapid rate of actuation is desired for quick wound occlusion.

The lack of sanitation in these high-risk war zones presents an additional challenge for treatment of open wounds [10]. The most common cause of infection in these environments is organisms such as gram-positive staphylococci and gram-negative rods [10]. To further enhance the utility of SMP foams for a wound application, honey-based phenolic acids are incorporated into the matrix to impart antimicrobial properties to the foams. Honey-based phenolic acids are known for their ability to inhibit bacterial and fungal growth [9]. For this study, cinnamic acid (CA) and phenylacetic acid (PAA) were selected due to their demonstrated antimicrobial activity and potential for incorporation into a polyurethane matrix. Both phenolic acids have been shown to inhibit growth of gram-positive Staphylococcus aureus and gram-negative Escherichia coli (E. coli), in addition to other strains of bacteria [11, 12]. Additionally, both acids have shown

efficacy in inhibiting the growth of fungi and biofilms [13]. Incorporating phenolic acids into polyurethane SMP foams could potentially produce foams that exhibit antimicrobial properties.

CHAPTER II

METHODS

Synthesis of Phenolic Acid Modified HPED Monomer

An esterification reaction was carried out by reacting the carboxylic acid group on the phenolic acids with an alcohol group on HPED. The reactions of CA and PAA with HPED produced N,N,N,N'-tetrakis(2-hydroxypropyl) ethylene diamine - cinnamic acid (HCA) and N,N,N,N'-tetrakis(2-hydroxypropyl) ethylene diamine - phenylacetic acid (HPAA), respectively. The expected chemical structures of these compounds can be seen in Figure 1.

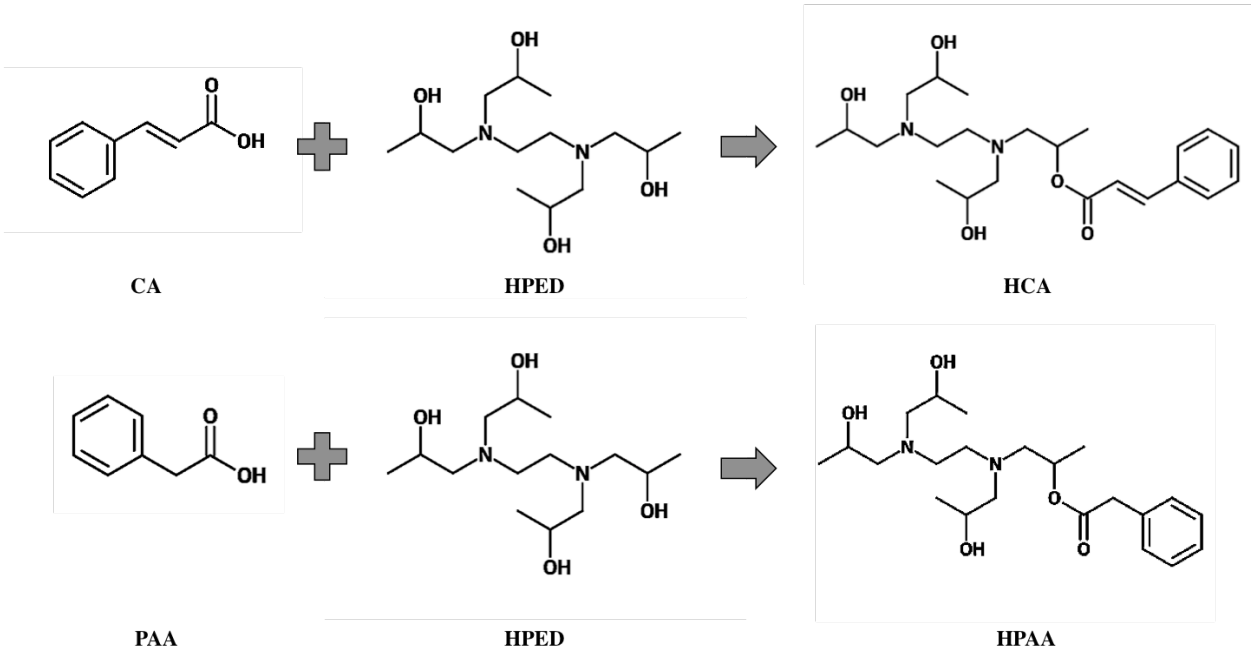

Figure 1. Esterification reactions of phenolic acids with HPED to form modified HPED monomers.

For each reaction, the respective phenolic acid (1 molar eq.) was added to a round bottom flask and dissolved in chloroform. 4-Dimethylaminopyradine (0.1 molar eq.) was then dissolved in the flask. HPED (1 molar eq.) was weighed in a separate container, dissolved in chloroform, and added dropwise to the solution. Similarly, N-N'-Dicyclohexylcarbodiimide (DCC) (1.1 molar eq.) was weighed, dissolved in chloroform, and added dropwise to the flask. The round bottom flask was then sealed with a rubber stopper and allowed to react at room temperature and under nitrogen flow for 3 hours.

When the reaction was complete, dicyclohexyl urea was precipitated by leaving the flask at 0°C for 30 minutes. Vacuum filtration was used to separate the dicyclohexyl urea from the reaction solution. The reaction solution was placed in a separatory funnel and washed with 0.1M hydrogen chloride (1 molar eq.) to remove the aqueous layer. The solution was then washed with a saturated sodium bicarbonate solution. The organic layer was dried in a magnesium sulfate solution. The magnesium sulfate was filtered via vacuum filtration and the remaining chloroform was removed using rotary evaporation. The solution was placed under vacuum overnight to dry.

Fourier Transform Infrared (FTIR) Spectroscopy

FTIR spectroscopy was used to confirm the synthesis of the HPED-phenolic acid monomers. A microliter pipette was used to spread the monomer over the surface of a potassium bromide disk. The disk was then dried in a bell jar for 10 minutes. The dried disk was placed in a Bruker Optics FTIR Spectrometer ALPHA (Bruker, Billerica, MA) where 32 background scans and 32 sample scans were performed in transmission mode with a 4 cm^{-1} resolution. OPUS software (Bruker,

Billerica, MA) was used to conduct a baseline correction and atmospheric compensation, and remove background scans.

Foam Synthesis

A pre-polymer mixture was prepared in a glove box by reacting an excess of diisocyanate groups in the form of hexamethylene diisocyanate (HDI) with 42 mol% of the total hydroxyl groups. The hydroxyl content was composed of 70wt% HPED and varying ratios of TEA and an HPED-phenolic acid monomer. These ratios are listed in Table 1 and Table 2. An additional foam was synthesized by directly incorporating CA into the pre-polymer mixture. The composition of this foam can be found in Table 1.

The pre-polymer mixture was cured under a heat cycle for 48 hours. The cured pre-polymer was then mixed with surfactants in a speedmixer. A second mixture was prepared by combining the remaining hydroxyl groups with deionized water and catalysts. The pre-polymer, hydroxyl mixture, and Enovate, a physical blowing agent, were then combined, mixed, and allowed to cure at 90°C for 5 minutes. The resultant foam was then cooled to room temperature for analysis.

Table 1. Foam compositions for CA series.

Sample Name	HDI (wt%)	HPED (wt%)	TEA (wt%)	HCA (wt%)	CA (wt%)
Control	100	70	30	0	0
HCA10	100	70	20	10	0
HCA20	100	70	10	20	0
HCA30	100	70	0	30	0
CA10	100	70	20	0	10

Table 2. Foam compositions for PAA series.

Sample Name	HDI (wt%)	HPED (wt%)	TEA (wt%)	HPAA (wt%)	PAA (wt%)
HPAA10	100	70	20	10	0
HPAA20	100	70	10	20	0
HPAA30	100	70	0	30	0

Densities

Foam densities were measured according to ASTM D3574-16. A resistive hot wire cutter was used to cut foam cubes (n=3) off sections of the main foam block free from defects. The length, width, and height of each piece were measured using a digital caliper. Densities were determined in terms of $g \bullet cm^{-3}$.

Pore Sizes

Thin slices of foam were taken from the axial and transverse axes of the main foam block. The slices were then mounted to a Scanning Electron Microscope (SEM) stub using carbon tape. The stub was placed inside a Cressington Sputter Coater (Ted Pella, Inc., Redding, CA) to undergo a gold sputter coating cycle with a current of 20mA for 60 seconds. The sample was then placed inside a Joel Neoscope JCM-5000 SEM (Nikon Instruments, Inc., Melville, NY) and imaged at 40X magnification. The resultant images were analyzed using ImageJ software (National Institutes of Health, Bethesda, MD). Pores (n=15) were measured along their major axis.

Thermal Transitions

To determine the dry T_g of each foam composition, dry foam samples (n=5, 5-10mg) were placed in Tzero Aluminum Hermetic Pans and sealed. The sealed pans were then placed in the

test well of a Q200 Differential Scanning Calorimeter (DSC) (TA Instruments, New Castle, DE) at room temperature. The samples were cooled to -40°C before being heated to 120°C at a rate of 10°C per minute. The temperature was held constant for 2 minutes and then lowered by 10°C per minute to -40°C. Again, the temperature was maintained for 2 minutes before returning to 120°C at a rate of 10°C per minute. The T_g was determined using TA Universal Software (TA Instruments, New Castle, DE) as the inflection point on the heat flow curve from the third cycle.

The wet T_g was determined by placing foam samples (n=5, 5-10mg) in 40°C reverse osmosis (RO) water for 10 minutes. The wet samples were set in the fold of a Kim Wipe (Kimberly-Clark, Roswell, GA) and placed in a Carver Press (Carver, Inc., Wabash, IN) to remove excess water. The mass of each wet sample was measured and the samples were sealed in Tzero pans. Each pan was vented and placed inside the test well of the DSC at room temperature. The samples were initially cooled to -40°C and held at this temperature for 5 minutes before being heated to 120°C at a rate of 5°C per minute. The wet T_g was found as the inflection point on the heat flow curve.

Volume Recovery

A 4mm biopsy punch was used to remove foam cylinders (n=3) from the main foam. A 254-micron nickel-titanium (nitinol) wire was threaded through the axial center of each foam cylinder. The wire was then placed inside an SC150-42 Stent Crimper (MSI, Flagstaff, AZ) heated to 100°C. The foam samples were heated for 15 minutes before they were crimped to 2mm at 50psi. The crimper was cooled, and the crimped foams were removed when the

apparatus reached room temperature. The samples were then stored in a dry environment for 24 hours.

After 24 hours, an RO water bath was heated to 37°C. The foam samples crimped on the nitinol wire were immersed in the water to begin thermal expansion. A digital camera was used to take images of the foams every 30 seconds for 7 minutes. An additional image was taken of the dry foams prior to thermal expansion for reference purposes. ImageJ software was used to take measurements (n=5) of the diameter of each cylinder at every time point.

Antimicrobial Properties

Polymeric films with compositions matching those of the foams outlined in Table 1 were cut using a 6 mm biopsy punch (n=3). The samples were soaked in phosphate buffered saline (PBS) at 37°C for 0, 10, 20, and 30 days. The films were sterilized overnight with 70% ethanol, and then washed with PBS 3 times to remove residual ethanol.

To begin preparation of the bacteria solution, E. coli and Staph. epi. were added to 5mL of lysogeny broth (LB) using an inoculation loop. The solution was then left overnight at 37°C. To obtain the desired log phase growth, 500μL of the solution were added to 10mL of sterile LB. The bacteria were allowed to grow until the desired optical density of 0.6 was reached. The optical density was confirmed using a Tecan Infinite M200 Pro Microplate Reader (Tecan Group Ltd., Mannedorf, Switzerland).

The polymeric film samples were each placed in a well of a sterile 96 well plate. 100μL of the bacteria solution was pipetted into each sample well. The samples were then kept at 37°C for 1 hour. The well plate was vortexed to ensure bacterial suspension. The solution was diluted by 10^6 using fresh LB and plated on sterile LB agar plates using an inoculation loop. The agar plates were then placed at 37°C overnight. Images of each plate were taken to determine the colony forming unit density. Densities were determined by counting the number of colonies and dividing by the area of the plate.

CHAPTER III

RESULTS

FTIR Spectroscopy

To confirm the synthesis of the HPED-phenolic acid monomers, the reaction products of the esterification reactions were analyzed using FTIR spectroscopy. Figure 2 shows the FTIR spectra for HCA, along with CA and HPED for comparison. Figure 3 provides a similar comparison for HPAA, PAA, and HPED.

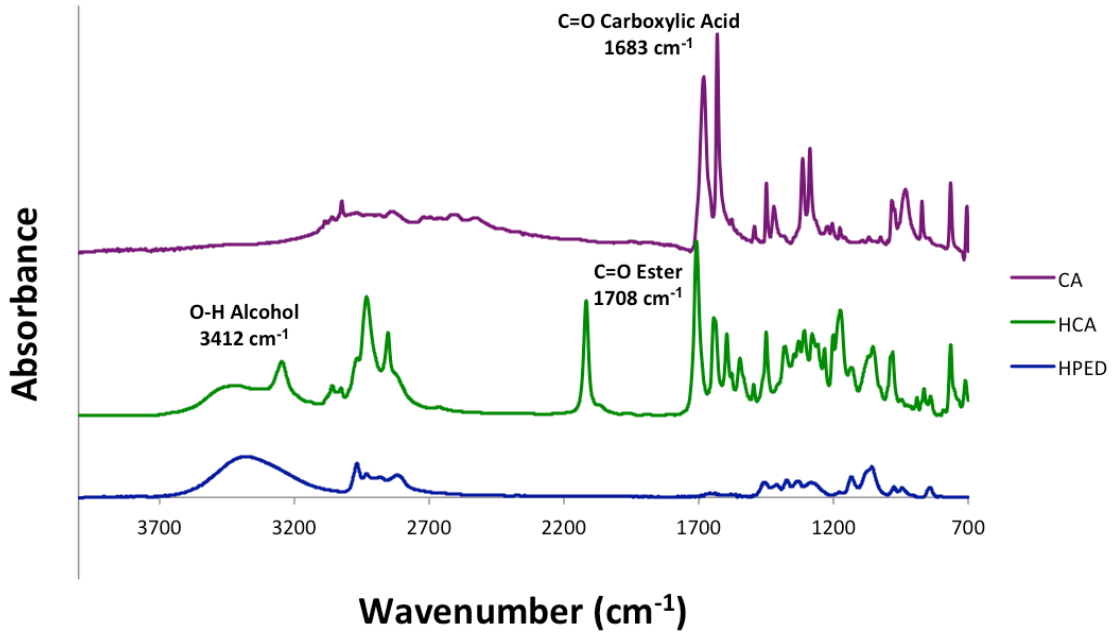

Figure 2. FTIR spectra comparing absorbance values for CA, HCA, and HPED.

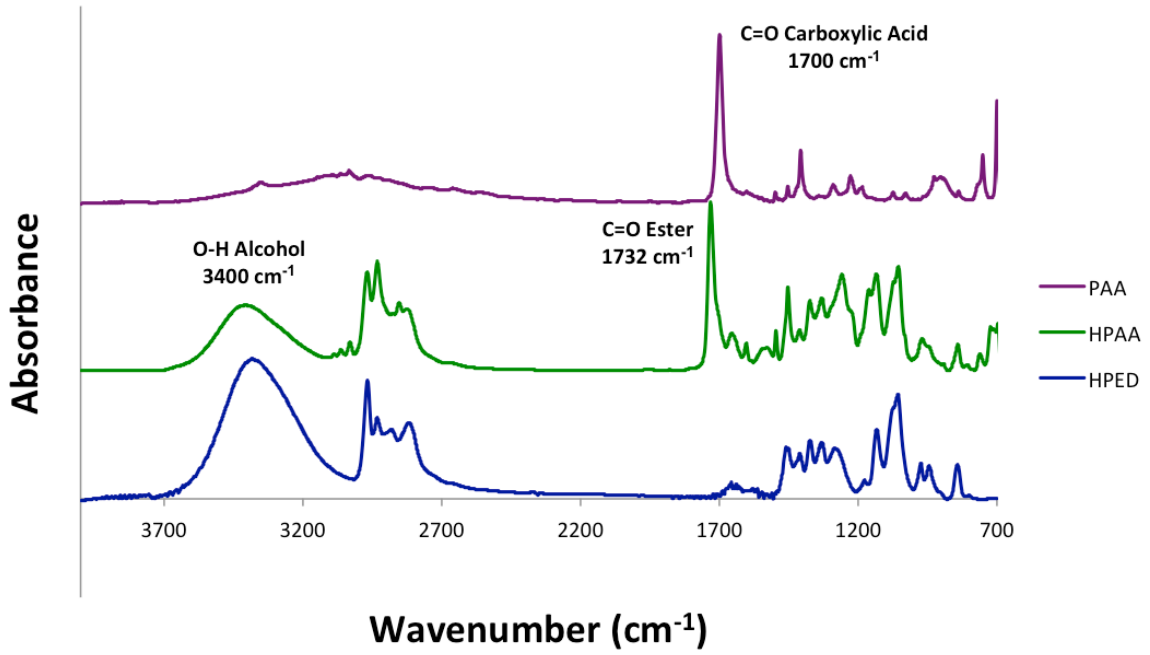

Figure 3. FTIR spectra comparing absorbance values for PAA, HPAA, and HPED.

In Figure 1, a carboxylic acid group can be observed on both CA and PAA. Peaks representative of these functional groups are present in the spectra of both CA and PAA between 1680 - 1700cm^{-1} (Figure 2 and Figure 3). During the esterification reactions, these carboxylic acids are converted to esters. This ester formation is confirmed by the shift of the carboxylic acid peak to an ester peak located around 1705 - 1735cm^{-1} in the spectra of both HCA and HPAA.

Additional confirmation can be found by comparing the alcohol peaks of HCA and HPAA with that of HPED. HPED is a compound containing 4 alcohol groups. During the esterification reaction shown in Figure 1, one of the alcohol groups on HPED was reacted with the carboxylic acid group from the phenolic acids. This resulted in reaction products containing 3 alcohol groups. This decrease in alcohol groups can be observed in the FTIR spectra as a reduction in the alcohol peak at approximately 3400cm^{-1} going from HPED to HCA and HPAA. The formation of ester peaks and reductions in the sizes of the alcohol peaks in both HCA and HPAA confirm

successful esterification reactions and synthesis of the modified HPED monomers, HCA and HPAA.

Densities

Densities for the CA and PAA series are reported in Table 3 and Table 4, respectively. For both series, the foams maintained the ultra-low densities found in the control and similar polyurethane SMP foams [6]. Among the foams containing HCA and HPAA, densities decreased with increased amounts of modified monomer.

Table 3. Densities for the CA series (n=3).

Sample Name	ρ (g•cm^{-3})
Control	0.0194 ± 0.0007
HCA10	0.0582 ± 0.0157
HCA20	0.0378 ± 0.0015
HCA30	0.0221 ± 0.011
CA10	0.0312 ± 0.0035

Table 4. Densities for the PAA series (n=3).

Sample Name	ρ (g•cm^{-3})
HPAA10	0.0419 ± 0.0015
HPAA20	0.0347 ± 0.0010
HPAA30	0.0293 ± 0.0040

Pore Sizes

As shown in Figure 4 and Figure 5, pore sizes in both the axial and transverse axes increased with increased amounts of modified monomer. This result follows the trend seen previously with foam densities. Larger pore sizes correspond to lower densities.

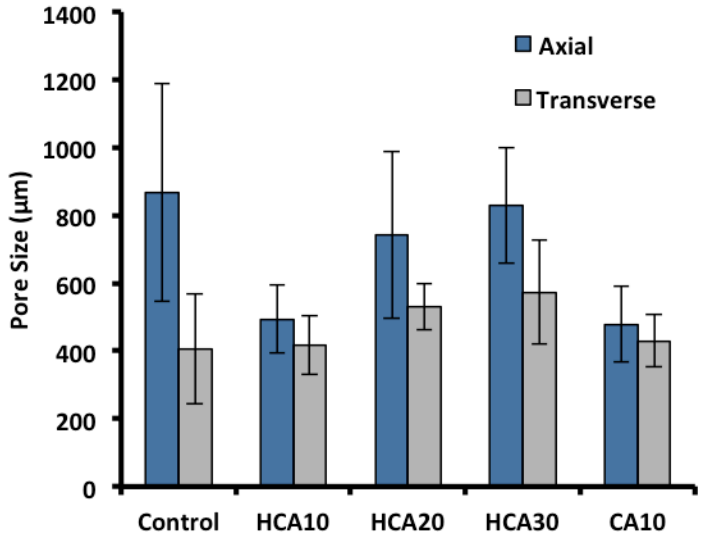

Figure 4. Axial and transverse pore sizes for CA series (n=15).

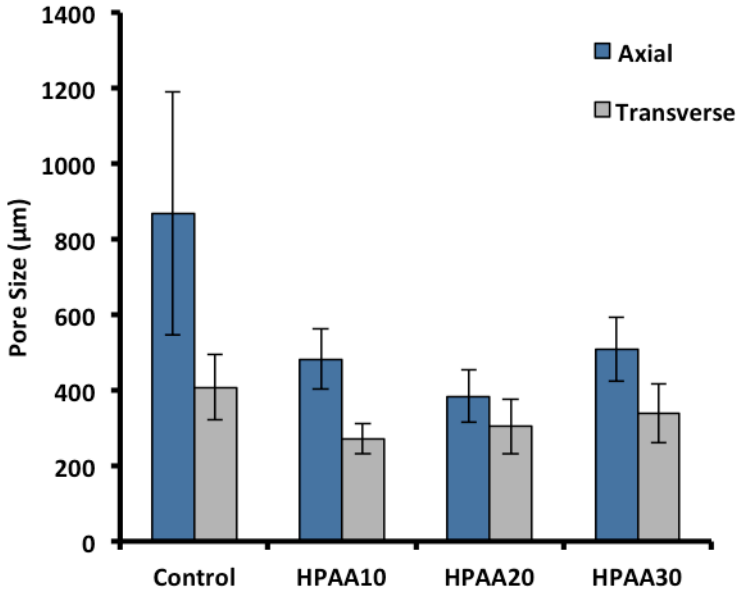

Figure 5. Axial and transverse pore sizes for PAA series (n=15).

The axial pores of HPAA10 and HPAA20 are an exception to this trend. It is possible the HPAA20 composition had less successful foam blowing compared to the other foam compositions, resulting in smaller pores in the axial direction. However, all foams exhibited good pore interconnectivity (Figure 6) confirming foam synthesis.

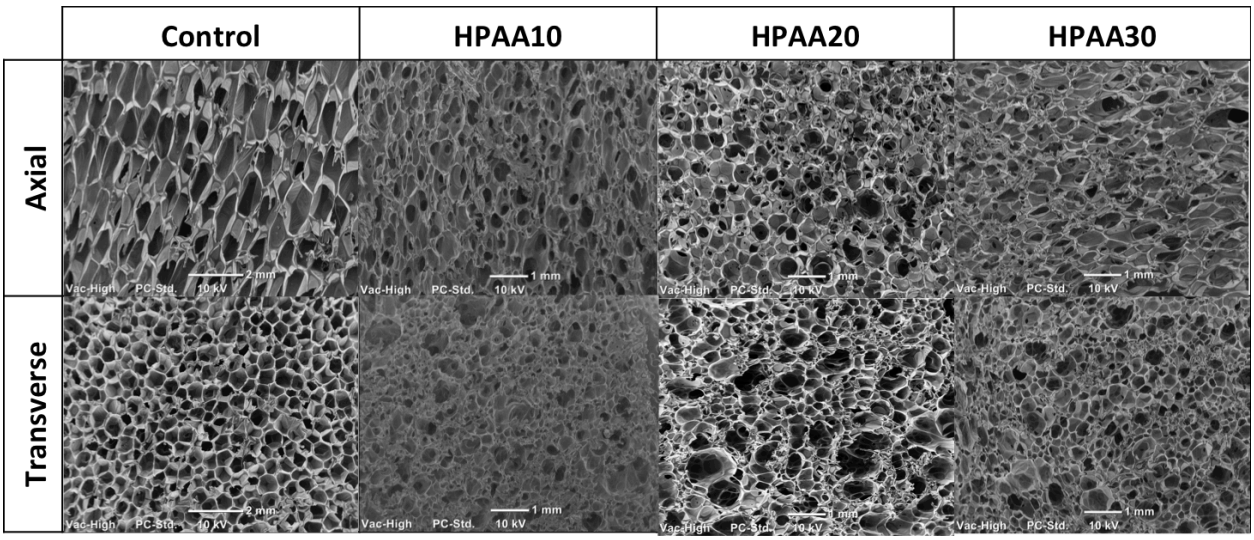

Figure 6. SEM images of axial and transverse pores for the PAA series.

Thermal Transitions

Polyurethane SMP foams are known to have different T_g's in dry and wet conditions. Figure 7 and Figure 8 show both dry and wet T_g's for the CA and PAA series, respectively.

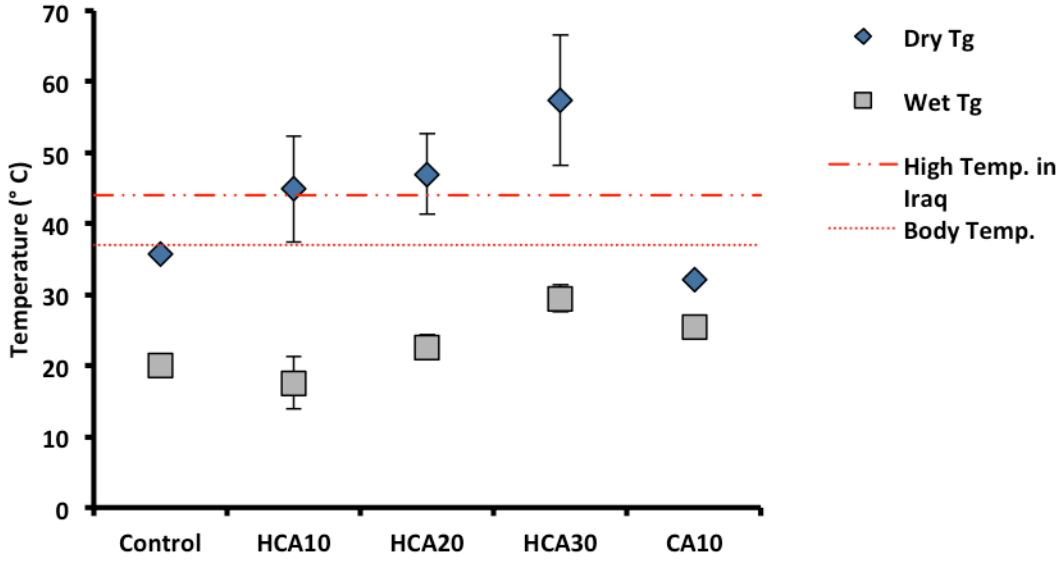

Figure 7. Dry and wet T_g's for HCA series (n=5).

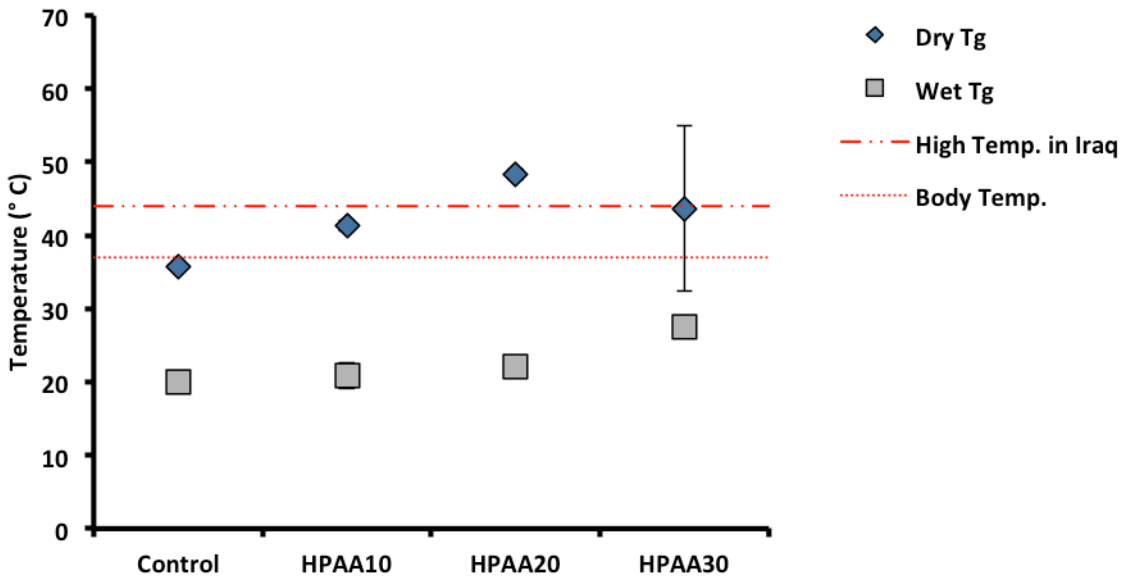

Figure 8. Dry and wet T_g's for HPAA series (n=5).

For the CA series, the dry T_g's increased with increased amounts of HCA. The chemical structure of HCA (Figure 1) is large and bulky. By increasing the concentration of this compound, more energy, and thus a higher temperature, must be applied to the polymer before it can rotate about its backbone. A similar trend was observed in the HPAA foams (Figure 8).

A wet T_g can be found after exposing a foam to an aqueous environment. When a polyurethane foam is exposed to water, the material is plasticized. Plasticization occurs when water molecules interrupt the hydrogen bonds in the material to weaken the foam matrix. A weaker matrix requires less energy to reach the T_g. Therefore, the wet T_g of a foam is lower than its respective dry T_g.

For both the CA and PAA foam series, the wet T_g's of the foams increased with increased amounts of HCA and HPAA. The addition of CA and PAA to HPED resulted in a hydrophobic

product. When this hydrophobic product was incorporated into the polyurethane foam, the ability of the material to be plasticized was reduced. This results in a higher wet T_g.

For this material to serve as a wound dressing and fully occlude a wound, it must expand when placed in the body. Due to the high concentration of water in the blood, the wet T_g will be the dominant thermal transition. Therefore, the wet T_g must be equal to or less than 37°C. As demonstrated in Figure 7 and Figure 8, the wet T_g's of all foams in both the CA and PAA series meet this requirement.

The environment in which this material will be used poses additional challenges. Current U.S. war zones include Iraq and Afghanistan. Both locations experience high temperatures that may cause premature foam actuation, thereby reducing the efficacy of the material. According to the World Meteorological Society, the mean daily maximum temperature in July in Baghdad, Iraq is 44.0°C [14]. Ideally, the dry T_g's of the foams would be above this value. However, only HCA30 and HPAA20 achieved this goal. Additionally, a foam may begin to expand at any temperature within about 5°C of the T_g value. This presents a risk of early expansion even for those foams that met the first requirement. Therefore, it would be necessary to identify a means for preventing foam actuation until device deployment. Humidity is another environmental challenge. As previously described, SMP foams become plasticized in aqueous environments and exhibit a decrease in their T_g. If these foams are used in humid environments, such as Vietnam, the foams may enter a rubbery state and expand prior to use. These considerations suggest that other methods, such as packaging should be designed to prevent premature actuation and plasticization of the foams.

Volume Recovery

All foams were placed in a 37°C water bath to simulate placement of the foam in the body. The expansion profiles shown in Figure 9 and Figure 10 demonstrate the rate at which the foams expanded under these conditions.

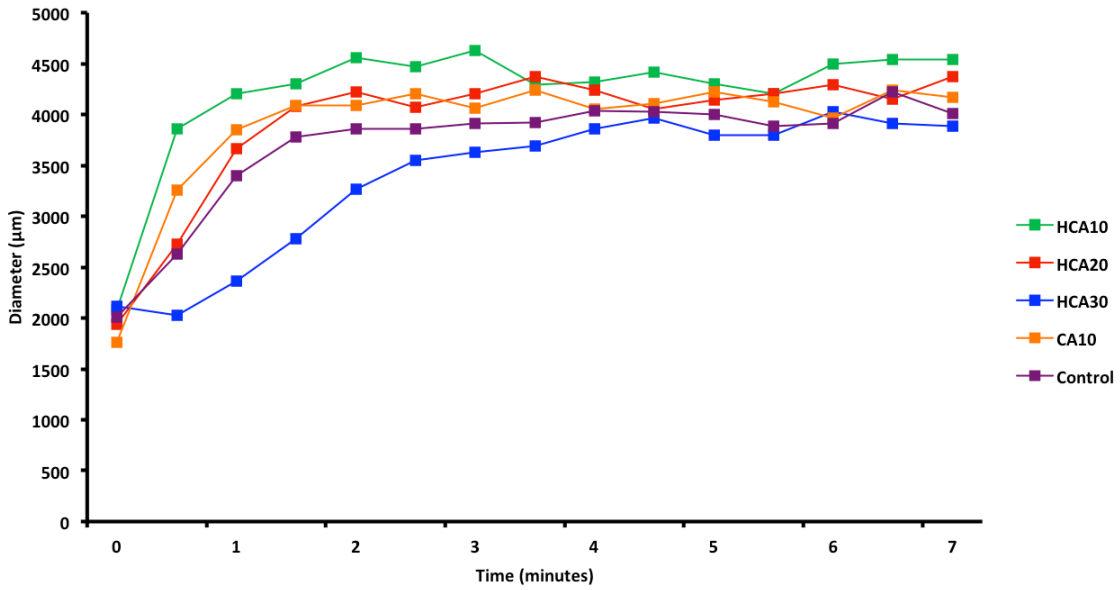

Figure 9. Expansion profiles for CA foam series (n=15).

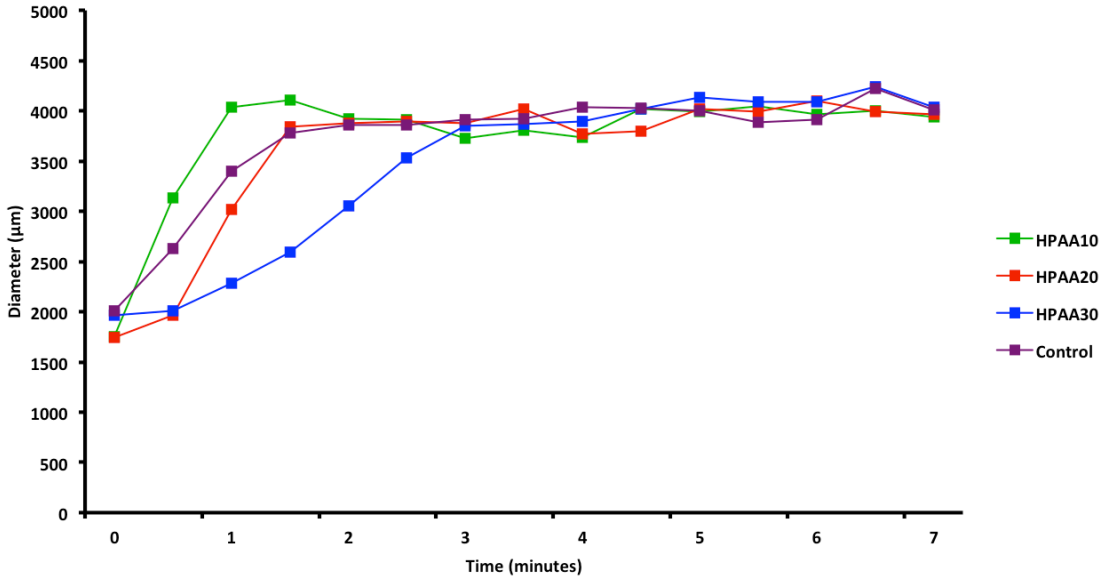

Figure 10. Expansion profiles for PAA foam series (n=15).

For both sets of foams, the rate at which the foams achieved full volume recovery was highest for foams with decreased amounts of modified monomer. This trend may be linked to the wet T_g's found in the previous section. As the amount of modified monomer increased, the wet T_g's of the foams also increased. A foam with a higher wet T_g is expected to expand at a slower rate than a foam with a lower wet T_g if both foams are exposed to the same thermal stimulus.

XStat by RevMedX is a current wound dressing treatment that injects several expandable cellulose sponges into a wound cavity to apply even pressure on all parts of the wound [4]. These sponges have been shown to fill the wound cavity within 20 seconds of application [15]. The polyurethane SMP foams studied here have a slower expansion rate. However, all of the foams achieve near complete volume recovery within minutes. The 10 and 20% modified monomer compositions show particular promise by fully expanding in less than 2 minutes, satisfying the need for rapid wound occlusion.

Antimicrobial Properties

The antimicrobial properties of the films were quantified in colony forming units (CFU) /cm^2. The results were compared to a negative control film with a composition matching the control foam found in Table 1 and a positive control of Penicillin/Streptomycin (P/S).

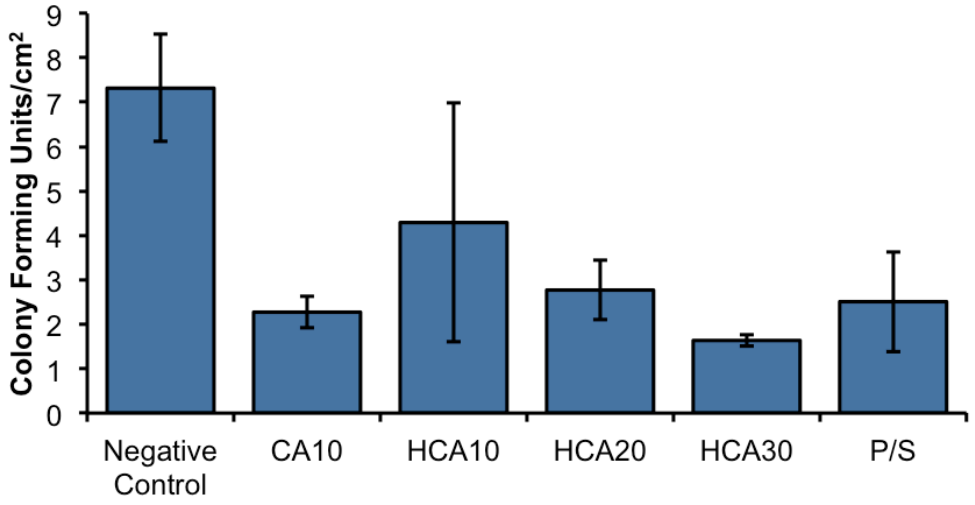

Figure 11. Antimicrobial effectiveness of CA series films against Staph. epi (n=3).

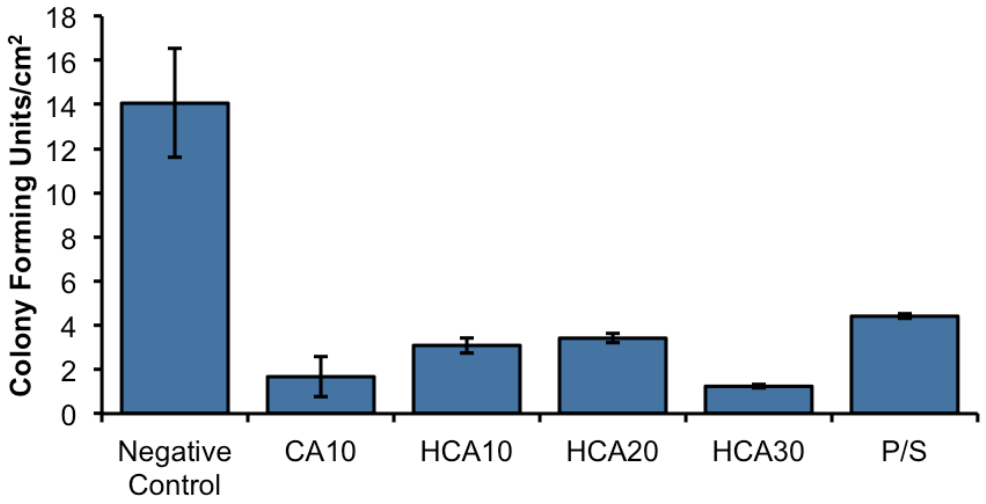

Figure 12. Antimicrobial effectiveness of CA series films against E. coli (n=3).

HCA30 was the most effective antimicrobial agent (Figure 11 and Figure 12). This result is likely due to the increased amount of modified monomer present in the film. CA10 also showed strong reductions in the CFU density. The direct incorporation of CA into the foam may have enabled more effective incorporation of the phenolic acid, leading to improved antimicrobial properties. All films had CFU densities less than that of the negative control. Additionally, all films except for HCA10 had CFU densities similar to or less than that of the positive control.

This indicates that the antimicrobial properties of CA were retained after the esterification reaction.

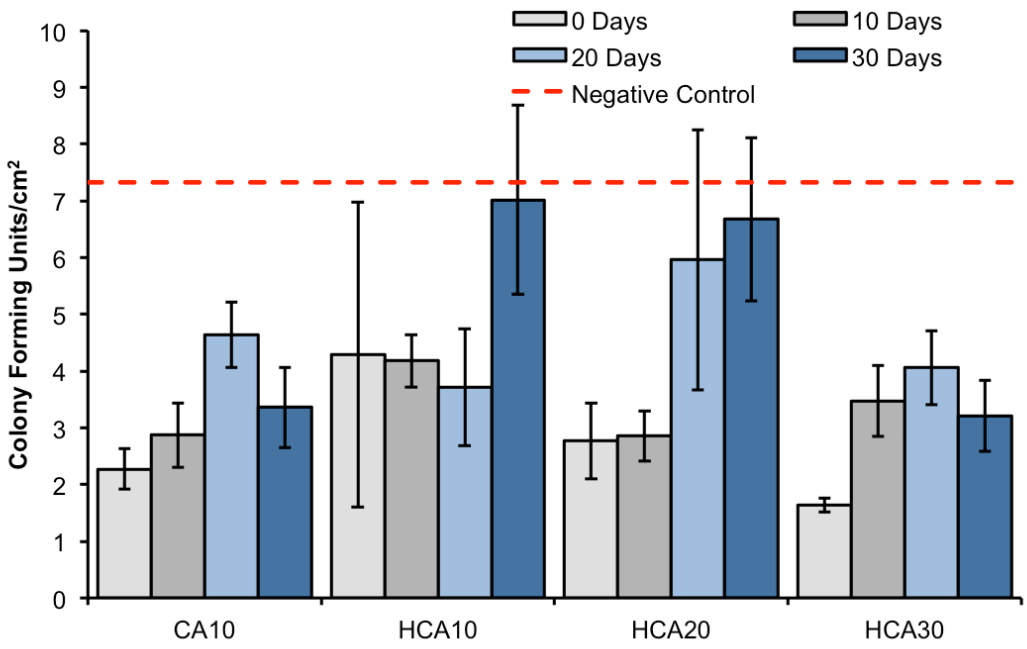

Figure 13. Antimicrobial effectiveness of CA series films against Staph. epi. after exposure to PBS over 0, 10, 20, and 30 days.

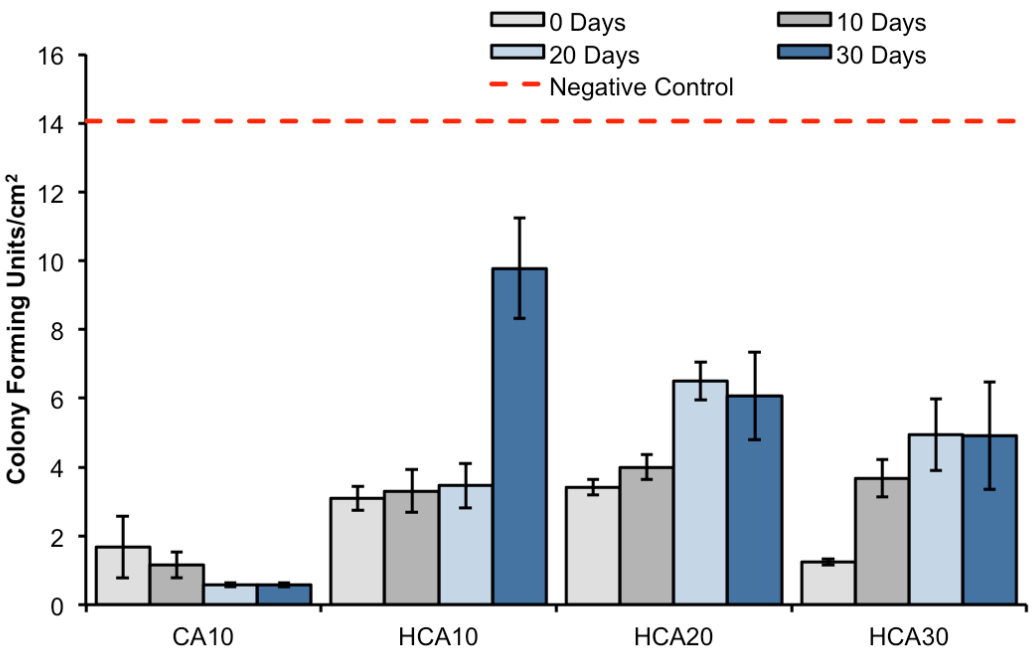

Figure 14. Antimicrobial effectiveness of CA series films against E. coli. after exposure to PBS over 0, 10, 20, and 30 days.

All film compositions were soaked in PBS solution for 0, 10, 20, and 30 days to identify how their antimicrobial properties might change after long term exposure to the body. Figure 13 and Figure 14 display the results. After 30 days, the HCA30 films remained the most effective among films containing HCA. However, all HCA films saw decreased antimicrobial effectiveness over the 30 days. During synthesis of HCA, an ester bond was formed to link HPED to CA. When placed in a PBS solution, this ester bond is susceptible to hydrolysis. Film degradation via hydrolysis would have resulted in films with lower HCA concentrations, which would be expected to show lower antimicrobial effectiveness.

To further evidence this hypothesis, the CA10 film, which did not contain an ester bond, remained effective after 30 days. When CA was incorporated into the polyurethane SMP film, a

urethane bond was formed. This bond is biostable. Therefore, it did not undergo the same degradation seen with the HCA films. Even after 30 days, all films were more effective at reducing the CFU density than the negative control.

CHAPTER IV

CONCLUSION

Honey-based phenolic acids, CA and PAA, were successfully incorporated into polyurethane SMP foams. An esterification reaction was carried out to modify a HPED compound. The resultant product was then incorporated into polyurethane SMP foams in varying amounts. Successful foam blowing was achieved and the foams maintained their characteristic ultra-low densities. The thermal transitions of the foams were analyzed. All of the foams exhibited wet T_g's below body temperature, enabling foam actuation when placed in a wound. The dry T_g's of the foams do not exceed all potential outdoor temperatures. While extreme heat poses a risk of premature foam actuation, specialized packaging may be developed to mitigate these risks. All of the foams achieved near complete volume recovery within minutes, suggesting a high potential for rapid wound occlusion. The incorporation of honey-based phenolic acids additionally imparted antimicrobial properties to the polyurethane foams. The foams were more effective than the positive control, Penicillin/Streptomycin, and could reduce the risk of infection for patients. In the future, antimicrobial testing will be performed on the PAA series to compare the antimicrobial properties of the foams to that of the CA series and the positive and negative controls.

REFERENCES

[1] Eastridge, Brian J., et al. "Died of Wounds on the Battlefield: Causation and Implications for Improving Combat Casualty Care." *The Journal of Trauma: Injury, Infection, and Critical Care*, vol. 71, no. supplement, 2011, pp. S4–S8.

[2] Kauvar, David S., et al. "Impact of Hemorrhage on Trauma Outcome: An Overview of Epidemiology, Clinical Presentations, and Therapeutic Considerations." *The Journal of Trauma: Injury, Infection, and Critical Care*, vol. 60, no. supplement, June 2006, pp. S3–S11.

[3] Alam, Hasan B., et al. "Hemorrhage Control in the Battlefield: Role of New Hemostatic Agents." *Military Medicine*, vol. 170, no. 1, Jan. 2005, pp. 63–69.

[4] Kragh, John F., et al. "Gauze vs XSTAT in Wound Packing for Hemorrhage Control." *The American Journal of Emergency Medicine*, vol. 33, no. 7, 2015, pp. 974–976.

[5] Boyle, Anthony J., et al. "In Vitroandin Vivoevaluation of a Shape Memory Polymer Foam-over-Wire Embolization Device Delivered in Saccular Aneurysm Models." *Journal of Biomedical Materials Research Part B: Applied Biomaterials*, vol. 104, no. 7, 2015, pp. 1407–1415.

[6] Singhal, Pooja, et al. "Ultra Low Density and Highly Crosslinked Biocompatible Shape Memory Polyurethane Foams." *Journal of Polymer Science Part B: Polymer Physics*, vol. 50, no. 10, Apr. 2012, pp. 724–737.

[7] Shubbar, Ramiz M., et al. "Characteristics of Climate Variation Indices in Iraq Using a Statistical Factor Analysis." *International Journal of Climatology*, John Wiley & Sons, Ltd, 11 May 2016.

[8] Singhal, Pooja, et al. "Controlling the Actuation Rate of Low-Density Shape-Memory Polymer Foams in Water." *Macromolecular Chemistry and Physics,* WILEY-VCH Verlag, 9 Oct. 2012.

[9] Guzman, Juan. "Natural Cinnamic Acids, Synthetic Derivatives and Hybrids with Antimicrobial Activity." *Molecules*, vol. 19, no. 12, 2014, pp. 19292–19349.

[10] Murray, Clinton K., et al. “Prevention and Management of Infections Associated With Combat-Related Extremity Injuries.” *The Journal of Trauma: Injury, Infection, and Critical Care*, vol. 64, no. Supplement, 2008.

[11] Kim Y, et al. (2004) Identification and Antimicrobial Activity of Phenylacetic Acid Produced by Bacillus licheniformis Isolated from Fermented Soybean, Chungkook-Jang. *Curr Microbiol* 48(4):312–317.

[12] Narasimhan B, Belsare D, Pharande D, Mourya V, Dhake A (2004) Esters, amides and substituted derivatives of cinnamic acid: Synthesis, antimicrobial activity and QSAR investigations. *Eur J Med Chem* 39(10):827–834.

[13] Teodoro GR, Ellepola K, Seneviratne CJ, Koga-Ito CY (2015) Potential use of phenolic acids as anti-Candida agents: A review. *Front Microbiol* 6(DEC):1–11.

[14] World Weather Information Service. (2018). *World Weather Information Service*. [online] Available at: https://worldweather.wmo.int/en/city.html?cityId=1464 [Accessed 3 Apr. 2018].

[15] REVMEDX. (2018). *XSTAT*. [online] Available at: https://www.revmedx.com/xstat [Accessed 4 Apr. 2018].